Scaling of nuclear numbers and their spatial arrangement in skeletal muscle cell size regulation

Kenth-Arne Hansson[a,*] and Einar Eftestøl[b]
[a]Section for Health and Exercise Physiology, Inland Norway University of Applied Sciences, 2624 Lillehammer, Norway;
[b]Department of Biosciences, University of Oslo, 0371 Oslo, Norway

ABSTRACT **Many cells display considerable functional plasticity and depend on the regulation of numerous organelles and macromolecules for their maintenance. In large cells, organelles also need to be carefully distributed to supply the cell with essential resources and regulate intracellular activities. Having multiple copies of the largest eukaryotic organelle, the nucleus, epitomizes the importance of scaling gene products to large cytoplasmic volumes in skeletal muscle fibers. Scaling of intracellular constituents within mammalian muscle fibers is, however, poorly understood, but according to the myonuclear domain hypothesis, a single nucleus supports a finite amount of cytoplasm and is thus postulated to act autonomously, causing the nuclear number to be commensurate with fiber volume. In addition, the orderly peripheral distribution of myonuclei is a hallmark of normal cell physiology, as nuclear mispositioning is associated with impaired muscle function. Because underlying structures of complex cell behaviors are commonly formalized by scaling laws and thus emphasize emerging principles of size regulation, the work presented herein offers more of a unified conceptual platform based on principles from physics, chemistry, geometry, and biology to explore cell size–dependent correlations of the largest mammalian cell by means of scaling.**

Monitoring Editor
Trina Schroer
Johns Hopkins University

Received: Sep 19, 2022
Revised: Mar 29, 2023
Accepted: Apr 28, 2023

INTRODUCTION

Size is a quantitative variable in biology that influences life on every scale. One such principal scale is the size of cells that in humans spans an extraordinary seven orders of magnitude in cell volume (Gillooly *et al.*, 2015).

Skeletal muscle cells are by far the largest mammalian cells, as human muscle fibers can have cross-sectional diameters of up to 100 µm (Kann, 1957) and span 45 cm in length (Harris *et al.*, 2005). Muscle fibers are syncytial cells, as they have a continuous cytoplasm that can contain many thousands of postmitotic nuclei dispersed along the surface within human muscle fibers (Hansson *et al.*, 2020a,b). Given these numbers, a typical human muscle cell has cytoplasmic volumes dimensionally equal to a spherical cell having a 1 mm radius and is thus twice the size of a frog oocyte (Wallace *et al.*, 1981) and 20 times larger than the approximately 0.05 mm human ovum (Xiao *et al.*, 2015), which is often incorrectly referenced for being the largest cell type in the human body. Herein, we discuss how these muscle cell–specific features adhere to the same scaling rules as mononucleated cells, establishing the boundaries for molecular dynamics and muscle fiber size regulation.

All cells need to distribute and transport molecular cargo within the cytoplasm by either diffusion or active transport, for which the diffusion time (t) scales to the cytoplasmic distance (L) approximately as $t \propto L^2$ (Luby-Phelps, 2013), while active transport scales linearly as $t \propto L$ (Soh *et al.*, 2013) (Figure 1). Therefore, the diffusion of a macromolecule to its target site is more strongly dependent on the cellular dimensions in comparison to active transport, causing molecules within a large cell to acquire unproportionally longer transport times relative to the increase in intracellular distances. Consequently, differences in intracellular dimensions cause small and large cells to work at different timescales (Cadart *et al.*, 2019; Hansson *et al.*, 2020b), which must be accommodated by numerically scaling networks of organelles and macromolecules according to the cell size for the purpose of maintaining its function at a given timescale.

DOI:10.1091/mbc.E22-09-0424
*Address correspondence to: Kenth-Arne Hansson (kenth.arne.hansson@inn.no).
Abbreviations used: EDL, extensor digitorum longus; MyHC, myosin heavy-chain; VEGF, vascular endothelial growth factor.

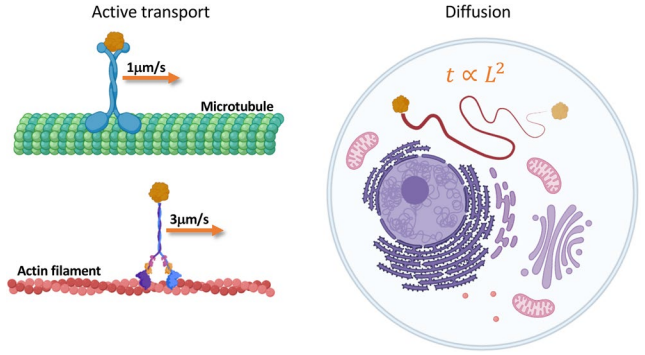

FIGURE 1: Intracellular transportation of macromolecules. Active transport along the cytoskeleton relies on the molecular motor protein transporting the cargo. Kinesins moving along microtubules typically move at a speed of 1 µm/s (Pilling *et al.*, 2006), while myosin V moves at a speed of 3 µm/s (Schott *et al.*, 2002). Diffusion time scales to the square of the distance traveled, causing diffusive transport of myoglobin within a fiber of the EDL muscle to be faster than actin-mediated transport for distances less than 25 µm and less than 75 µm relative to transportation along microtubules (Hansson *et al.*, 2020b).

A major tenet in muscle biology has been concerning synthetic capacity and transportation within muscle fibers (Cheek, 1985; Bruusgaard *et al.*, 2003; Manhart *et al.*, 2018). The multinucleation of muscle cells inspired Cheek and coworkers to conceptualize the theory of a DNA unit (Cheek *et al.*, 1971), which is also identified as a myonuclear domain (Hall and Ralston, 1989; Pavlath *et al.*, 1989; Allen *et al.*, 1999), defining the theoretical amount of cytoplasm supported by a single nucleus. Muscle fibers are made up of many myonuclear domains, and their number and size may thus be a proxy for physical limitations of transport and biosynthetic capacity within domain boundaries. A more detailed investigation of myonuclear domain properties and their relation to cellular transport limitations through a scaling perspective may therefore aid in our understanding of how muscle fiber size is regulated.

SCALING CELLULAR QUANTITIES WITH SIZE

Scaling relationships quantitatively describe how measurable properties of the cell *scale* with size. The underlying manifestation of size stems from the numerous growth pathways that convey extracellular cues and intracellular signals to balance the rate of synthesis and degradation of proteins (Gundersen, 2011; Schiaffino and Reggiani, 2011; Kafri *et al.*, 2016; Lin and Amir, 2018; Cadart *et al.*, 2019), while the integration of the numerous subunits of macromolecules and organelles is required to supply the cell with metabolic substrates and regulate activity according to size. For a cell to accommodate the greater functional need caused by its increase in size, it must therefore scale its number of organelles and macromolecules with its size to maintain function (Li *et al.*, 2014; Cadart *et al.*, 2019; Bertaux *et al.*, 2020; Hansson *et al.*, 2020a). The type of scaling can be reported by analyzing correlates of size by reporting the scaling parameter b in a power function of the form $y = ax^b$, causing the relationship to be either constant ($b \approx 0$), linear ($b \approx 1$), sublinear ($0 < b < 1$), or superlinear ($b > 1$). Recognizing the type of relationship may thus formalize underlying metabolic requirements and cellular pathways of size regulation, which have turned out to be instrumental in shaping our understanding of cell size regulation and homeostasis in many cell types (Mitchison, 2003; Chan and Marshall, 2010; Goehring and Hyman, 2012; Marguerat and Bahler, 2012; Niklas, 2015; Amodeo and Skotheim, 2016; Cadart *et al.*, 2018, 2019; Bertaux *et al.*, 2020; Hansson *et al.*, 2020a; Lanz *et al.*, 2022).

The domain volume of muscle fibers from the human v. lateralis muscle is volumetrically similar to that of megakaryocytes, but megakaryocytes are additionally supported by six times the DNA content (Ishibashi *et al.*, 1986), rendering human muscle fibers rather DNA scarce in comparison to the polyploid megakaryocyte (Hansson *et al.*, 2020a). The vast cytoplasmic volume within skeletal muscle fibers is therefore orchestrated by a relatively small number of DNA molecules, perhaps related to slower turnover rates compared with megakaryocytes. In large cells, like the skeletal muscle fiber, these organelles therefore need to be rather homogeneously distributed to efficiently supply the cytoplasm with metabolic substrates in mammals (Bruusgaard *et al.*, 2003; Hansson *et al.*, 2020a,b) and arthropods (Manhart *et al.*, 2018; Windner *et al.*, 2019).

The use of nuclei as the heuristic origin of a transportation network and their domain sizes may therefore represent underlying physical constraints on the synthetic capacity and intracellular transport efficiency. Connecting the correlates of size (e.g., mRNA and protein content) with the scaling of skeletal muscle networks (i.e., the distribution and number of organelles) may thus represent underlying mechanisms of size regulation.

DNA CONTENT SCALES IN DIRECT PROPORTION TO FIBER SURFACE AREA

A long-standing scaling law is that DNA content is linearly proportional to "size" for cells that contain more than two sets of chromosomes (polyploid). Hence, a diploid cell is twice the size of a smaller haploid cell, while a tetraploid cell is four times the size of a haploid cell (Rhind, 2021). The type of scaling, however, depends on the definition of "size" itself, which could be measured geometrically as length, area, and volume or as more indirect measures, such as total cell mass and transcription and protein content. One of the main reasons for this is that the composition and shape of cells can change independently of each other, so that associations between, for example, geometrical parameters and DNA content can significantly revise interpretations of size-related correlations (Miettinen *et al.*, 2017).

For most living systems, the scaling between an object's surface area and volume is expected to scale as a power law with an exponent of two-thirds (McMahon and Bonner, 1983; Schmidt-Nielsen, 1984), axiomatically causing the nuclear number regressed on fiber volume to display a nonlinear relationship if there is a linear relationship between the nuclear number and the fiber's surface area. Cells may, however, adopt a different geometric scaling that changes their shape. Such geometric dissimilitude may occur through elongation, flattening, or fattening of the cell, causing the scaling exponent to take on numbers larger or smaller than the expected two-thirds power from Euclidean scaling (Okie, 2013). For example, much information about the relationship between DNA content and cell size control has been based on studies performed using fission yeast (Cantwell and Nurse, 2019), which have shapes like a prolate spheroid that grows only by elongation along their longitudinal axis while keeping their girth fixed, causing their volume to be linearly related to their surface area (Chan and Marshall, 2010). Furthermore, more recently, DNA content and ploidy within the muscle fibers of the *Drosophila* larvae were found to scale in direct proportion to cytoplasmic volume (Windner *et al.*, 2019). However, the muscle fibers of *Drosophila* larvae are flat rectangular cells (Windner *et al.*, 2019), and their size adjusts merely in two dimensions (the width and the length) (Kim and O'Connor, 2021) while keeping the height of their fibers fixed, causing their surface area and volume to

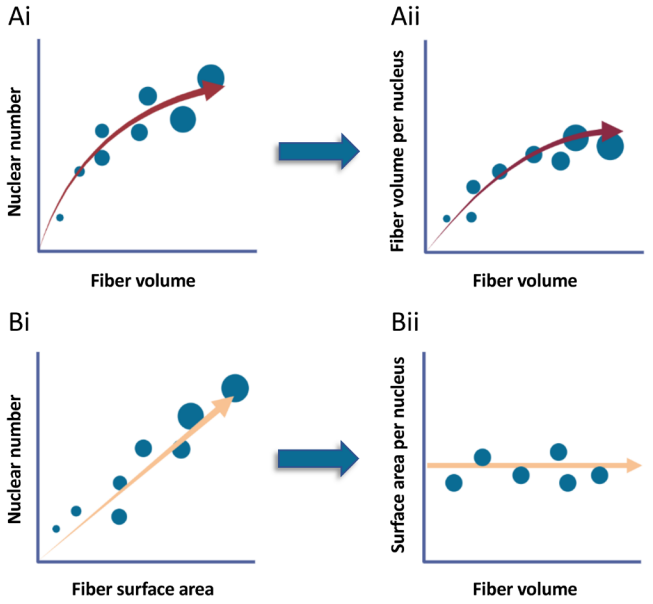

FIGURE 2: Nuclear number scales in direct proportion to the surface area. (Ai) DNA content (nuclear number) regressed on fiber volume displays a sublinear relationship with a scaling parameter close to two-thirds. This results in a scaling where the fiber volume per nucleus increases sublinearly as the fiber grows larger (Aii). (B) On the contrary, there is a linear relationship between the fiber surface area and DNA content (nuclear number), causing the surface area per nucleus to be constant as the volume of the fiber increases (Bii), which may signify an interdependence between the plasma membrane and myonuclear productivity (see text for further information).

be size proportional. Therefore, plotting the total amount of DNA against either the surface area or the cell volume would produce a linear relationship. On the other hand, when analyzing the relationship between cell size and genome content using the cell volume for 19 different human cell types, the genome content did not increase linearly but sublinearly with cell volume (Gillooly *et al.*, 2015), as expected if DNA content scaled in direct proportion with the surface area of a spherical cell. This also holds true for the multinucleated skeletal muscle fiber, as the number of diploid cell nuclei scales sublinearly with fiber volume but linearly with the fiber surface area (Hansson *et al.*, 2020a) (Figure 2).

It seems reasonable to explain size restrictions on the basis of cytoplasmic volume, because molecules and organelles occupy a three-dimensional space. Therefore, it has been suggested that DNA content can restrict size, which implies a mechanism present to measure cell size by the amount of DNA per volume (Padovan-Merhar *et al.*, 2015). In terms of scaling, one such mechanism would be if the amount of DNA and cell volume fail to keep a one-to-one pace, causing the DNA itself to become limiting to sustain transcription following cytoplasmic dilution (Demidenko and Blagosklonny, 2008; Miettinen and Bjorklund, 2016; Neurohr *et al.*, 2019).

However, because the ability of a fiber to exchange metabolic resources across the membrane is a function of a fiber's surface area, whereas the requirement for chemical energy is proportional to the cytoplasmic volume being metabolically maintained, one might assume that the transport rate of metabolic resources across the cell membrane is limited by the total surface area. Therefore, the supply of nutrients to fuel transcription and translation as fibers increase in size scales in direct proportion to the fiber perimeter for a muscle fiber of constant length, while the demand scales commensurate with the cross-sectional area. Hence, a large fiber is more constrained by its ability to acquire essential resources across the plasma membrane compared with a small fiber. In addition, one might further assume that the maximal and minimal fluxes of essential resources across the fiber surface set the upper and lower limits to myonuclear production rates. The constraints exerted by the fiber surface area on the myonuclear production capacity also impact the ability of each myonucleus to produce content for the plasma membrane, which may indicate that the nuclear production rate for substances being allocated toward the plasma membrane is narrowly tuned. This kind of reciprocity may be the physiological manifestation causing the nuclear number and fiber surface area to scale linearly with each other.

SPATIAL SCALING OF MUSCLE FIBER NETWORKS AND MYONUCLEI

From ecological communities to cities, designing spatial distribution networks to minimize mean distances between, for example, schools, parks, gas stations, and supermarkets is implicated in reducing the overall cost to maintain and build the networks, but also by effectively reducing the traveling distance for the citizens to reach their destination (Gilarranz, 2020). In biological terms, cellular networks emanate as a consequence of the functional hierarchy between DNA, RNA, protein, and smaller molecules within distribution pathways and their subsequent multifarious interactions, giving rise to cellular behavior (Albert, 2005). The diffusive transport distance and thus time depend on the structure and size of the molecule, for which mRNAs and proteins differ, causing the diffusion rate of the larger precursor polymer-like mRNA to be much slower than that of the translated protein. For example, the 45 kDa large ovalbumin injected within muscle fibers from the rat soleus muscle displays a diffusion coefficient of about 5 $\mu m^2/s$ (Papadopoulos *et al.*, 2001). On the contrary, the 380 kDa–sized β-actin mRNA has a diffusion coefficient measured to be 0.1–0.4 $\mu m^2/s$ within mouse embryonic fibroblasts (Katz *et al.*, 2016). Interestingly, ovalbumin and the β-actin protein (47 kDa) are size equivalent, theoretically causing the β-actin protein to travel the same diffusion distance 17 times faster compared with its mRNA precursor. The reason for this is that it takes three nucleotides to code for a single amino acid, while the approximately 330 Da nucleotides of the RNA (Dolezel *et al.*, 2003) have on average a mass three times heavier than the mass of an average 110 Da amino acid (Spahr, 1962), which causes the protein molecule to be one-ninth the size of the coding mRNA precursor.

Physical differences between mRNAs and proteins influencing their diffusion properties might explain why mRNAs are typically found close to the transcribing nucleus within muscle fibers (Merlie and Sanes, 1985; Hall and Ralston, 1989; Pavlath *et al.*, 1989; Ralston and Hall, 1992; Nevalainen *et al.*, 2013). In addition to the relative difference in size between mRNA and proteins, the aggregation of ribosomes and complexes of mRNA binding proteins with transcripts causes a further hindrance in mRNA transport rates due to the total increase in size (Katz *et al.*, 2016), plausibly causing the subcellular distribution of mRNA within muscle fibers to depend on microtubule-based transport in addition to diffusion (Denes *et al.*, 2021; Pinheiro *et al.*, 2021). On the contrary, proteins are spread over a greater distance within the fiber (Mishra *et al.*, 2015; Taylor-Weiner *et al.*, 2020), but the dense mesh of myofibrils impedes the diffusion of larger proteins as well (Papadopoulos *et al.*, 2000). It is therefore suggested that diffusive flux limits fiber size, partially because intracellular diffusion distances increase with fiber size, as the average myonuclear domain volume was recently shown to increase with fiber size (Hansson *et al.*, 2020a).

In addition, the peripheral localization of myonuclei per se causes the average cytoplasmic transport distances of gene products to the center of the fiber inevitably to increase with fiber size. However, the peripheral multinucleation of fibers also enables the nuclei to be close to the plasma membrane, the site that needs to be sustained at the fastest pace. For instance, the numerous proteins in the plasma membrane have a relatively short half-life, about 2–8 h (Beardslee *et al.*, 1998; Egger *et al.*, 2005; Di Biase *et al.*, 2011). On the contrary, sarcomeric proteins have half-lives ranging from 3 to 10 d (Zak *et al.*, 1977; Isaacs *et al.*, 1989; da Silva Lopes *et al.*, 2011), whereas the skeletal muscle myosin heavy-chain (MyHC) has a half-life of up to 30 d (Kay, 1978). Hence, essential structures within the fiber must be nurtured at different rates based on protein species and their turnover rates. Therefore, adequately distributing myonuclei spatially along the fiber surface becomes increasingly important with increasing fiber size, as nuclear mispositioning is associated with impaired muscle function (Cristea *et al.*, 2010; Folker and Baylies, 2013; Roman and Gomes, 2018).

Spatial Arrangement of Myonuclei to Optimize the Allocation of Cell Resources

For simplification, the measurement of nuclear spacing could be addressed in terms of a two-dimensional space, with reference to the fiber´s surface area (Bruusgaard *et al.*, 2003; Hansson *et al.*, 2020b). The distance from an individual nucleus to its nearest neighbor provides one basis for measuring nuclear spacing. Theories about similar patterns arising in population ecology have been previously derived (Clark and Evans, 1954) and are herein adapted with suitable modifications to be applicable to investigate spatial relationships of nuclei within muscle fibers. Hence, if the nuclei were randomly distributed along the fiber surface, the expected mean distance (d) between nuclei could be approximated based on the average cell membrane surface area per nucleus (D_S) according to the expression $d = 0.5\sqrt{D_S}$. On the other hand, nuclei become maximally spaced if they were arranged in a hexagonal pattern, resulting in a mean distance equal to $d = 1.075\sqrt{D_S}$, causing myonuclei evenly spaced to have internuclear distances being 2.15 times as large compared with the average distance observed when nuclei are arbitrarily placed along the surface of the fiber plasma membrane. Although the distance between nuclei is maximized under conditions that make them adapt to a theoretical hexagonal pattern, this in fact minimizes the mean transport distance to points along the surface when viewing every single nucleus as the origin of a transportation network within skeletal muscle fibers of mice (Hansson *et al.*, 2020b).

When spatial relationships were measured within fibers of the extensor digitorum longus (EDL) and soleus muscle of mice, the nuclei in the EDL were distributed close to optimally, while the positioning of the nuclei in the soleus fibers resembled more of a random distribution (Hansson *et al.*, 2020b). Overall, soleus fibers exhibited smaller domain sizes and shorter transport distances compared with EDL fibers and we found minimal improvement in reducing transport distances when placing nuclei optimally in the soleus fibers.

Different nuclear arrangements may thus suggest fiber size–dependent adaptations related to, for example, fiber type and metabolic rate, allowing both sufficient cross-talk between nuclei and transportation of molecules to all parts of the fiber. This is in tune with a recent study by Taylor-Weiner *et al.* (2020), where a model to create myotubes that contained exactly one nucleus expressing a fluorescent nuclear reporter showed that neighboring nuclei were able to import nuclear proteins up to a distance of 50 µm from the transfected nucleus, about twice the size of the average surface transport distances observed in the mature EDL muscle (Hansson *et al.*, 2020b). Transport distance was highly influenced by neighboring nuclear import rates that functioned as molecular sinks (Taylor-Weiner *et al.*, 2020), constraining the traveling distance of molecules. Another recent study using reporter mice in which dystrophin was tagged with EGFP in a subset of myonuclei showed that the distribution of dystrophin was defined as sarcolemmal domains of about 80 µm from the nucleus of origin (Morin *et al.*, 2023). Functionally, the spatial arrangement of myonuclei may be a combination of their ability to support muscle fibers with essential products and to reduce the time required for the exchange of gene products between nuclei.

Likewise, one might expect that nuclei are arranged according to the size of the fiber they occupy to accommodate for the greater transport distance observed as the fiber size increases. Similar problems have been addressed to scale the number of facilities, such as schools, hospitals, and supermarkets, according to differences in population density. Gastner and Newman (2006) found that the ideal solution to this problem is not to scale the number of facilities in direct proportion but to the two-thirds power of population density. In contrast, Hansson *et al.* (2020a) found that the nuclear number increased in direct proportion to the area of the fiber plasma membrane, causing each nucleus to serve a constant proportion of the surface area between fibers of various sizes. This metric also portrays that the average transport distances along the surface were fixed, invariably occurring both during muscle development and in muscle from adult mice, as well as in adult human muscle (Hansson *et al.*, 2020a). Nuclei thus seem to be positioned to minimize transport distances along the fiber surface, but the linear relationship between the nuclear number and the surface area translates into a scaling relationship that causes the nuclear number to scale sublinearly with fiber volume (Hansson *et al.*, 2020a). The effect of this is twofold. First, cytoplasmic transportation distances increase with fiber size, and second, each nucleus must produce a larger number of molecules to accommodate the larger myonuclear domain volumes, and as is discussed further below, this might be specifically related to regulation of the DNA content and growth rates.

GROWTH RATES ARE PROPORTIONAL TO THE DNA CONTENT PRESENT IN SKELETAL MUSCLE FIBERS

Most studies on cell growth investigate cells that typically divide, and therefore their average size and growth rate are determined by how much they grow between two division events (Chan and Marshall, 2010; Goehring and Hyman, 2012; Amodeo and Skotheim, 2016; Cadart *et al.*, 2018). Cell division thus offers an opportunity for size adjustment, for which nondividing cells cannot rely on. Instead, the relative rate of synthesis to degradation of proteins is therefore a key determinant of fiber size. The consequence of this type of regulation is that there could be significant size gains even when protein synthesis is reduced if there is an even more noticeable reduction in protein degradation (Miettinen and Bjorklund, 2015).

It has long been known that muscle fiber growth can be prevented by inhibiting RNA synthesis (Goldspink, 1977), and because about 80% of the cell's total RNA is rRNA, the total RNA represents a proxy for the de novo synthesis of ribosomes, mirroring the fiber´s total production capacity (Figueiredo and McCarthy, 2019; von Walden, 2019). Additionally, skeletal muscles respond rapidly to new functional requirements at the transcriptional level, whereas the response to synthesize and accumulate protein is slower (Andersen and Schiaffino, 1997; Andersen *et al.*, 1999). This seems to parallel the behavior in yeast strains caused by the delay between mRNA

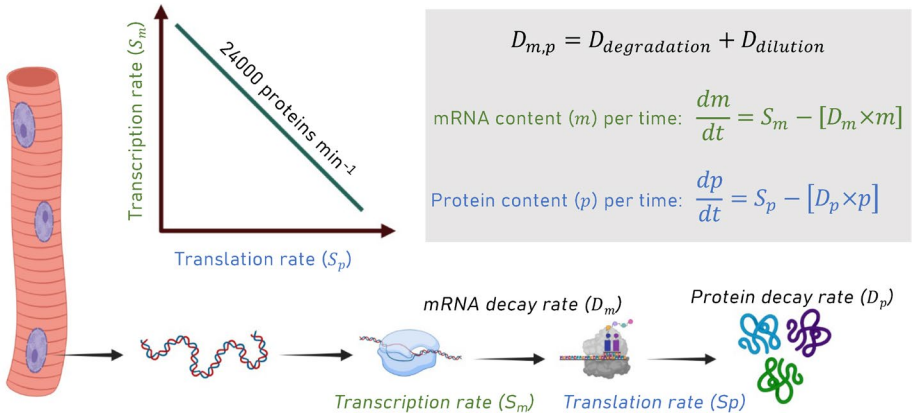

FIGURE 3: Myonuclear plasticity space. The protein content for each gene can be achieved by combining the transcription and translation rates of mRNA and proteins, respectively, as well as their corresponding decay rates. The decay rates for mRNA (D_m) and protein (D_p) are the sum of their degradation rates and the dilution at a rate of h^{-1} during the growth of muscle fibers. Activation and signaling of growth pathways from the extracellular space can modulate each of these microstates, causing an unlimited number of ways to cross-combine the four microstates coupled to each of the numerous proteins to maintain steady-state fiber size (grand macrostate). For example, signaling via myostatin leads to activation of the Smad2/3 pathway, causing overall proteolysis within muscle fibers (Sartori *et al.*, 2009), and thus influences D_p, while S_p and D_p are regulated by the extracellular cues mediated by the IGF-1 that leads to intracellular activation of the Akt/mTOR pathway that causes a net protein accumulation by promoting protein synthesis and inhibiting proteolysis (Schiaffino and Mammucari, 2011).

maturation and subsequent protein translation (Lee *et al.*, 2011). In other words, there is a positive correlation between the mRNA copy number, translation rate, and protein content (Marguerat and Bahler, 2012).

It is important to note that the protein copy number observed in steady-state is balanced between the transcription and translation rates and counterbalanced by the two rates of degradation as well as dilution of mRNAs and proteins (Hargrove and Schmidt, 1989). Consequently, the physical manifestation of each protein is regulated by a four-dimensional rate space, which herein is conveniently defined, on a per-nucleus basis, as the myonuclear plasticity space. The abundance of each protein (the macrostate) could thus be achieved in numerous ways by combining different rates (the four microstates). Mathematically, we may express the content of a single protein species P_i as follows:

$$P_i \approx \frac{S_m \times S_p}{D_m \times D_p}$$

where the synthesis rate (S) of transcription and translation is given by S_m = mRNA min^{-1} and S_p = protein min^{-1}, respectively. The decay (D) of mRNA and protein is given by the dilution and degradation of mRNA (D_m = mRNA min^{-1}) and protein (D_p = protein min^{-1}).

The skeletal muscle MyHC, which in muscle cell culture is estimated to be produced at rates of about 24,000 molecules min^{-1} $nucleus^{-1}$ (Young and Schneible, 1984), can thus be made, for example, by either transcribing 24 mRNAs and translating 1000 proteins per mRNA each minute or translating the astonishing 24,000 proteins from a single mRNA every minute (Figure 3).

Supporting the notion that the translation and saturation of ribosomes on the mRNAs become limiting to increase more abundant proteins in the cell (Schwanhausser *et al.*, 2011), it has also been pointed out that it is much more expensive for cells, based on an energy cost per protein, to up-regulate the synthesis of proteins of high abundance, relative to proteins of lower abundance (Liu *et al.*, 2016). This is in part because cells that transcribe highly expressed genes do so at close to maximal rates, leaving the burden and energy cost of optimizing the high protein content for cellular function at the level of ribosomal translation (Metzl-Raz *et al.*, 2020; Zur *et al.*, 2020).

In muscle fibers, the myofibrillar protein content accounts for the larger proportion of the total abundance of proteins, while the remaining proportion of proteins are sarcoplasmic (Fiorotto *et al.*, 2000). It could therefore be envisaged that it is less expensive for the fiber to globally increase the abundance of myofibrillary proteins and their precursors by allocating the synthetical burden between the nuclei in a supernumerary fiber, contrary to forcing individual nuclei to exceed their optimal production rate. Donating nuclei from muscle stem cells during overload-induced muscle growth before hypertrophy (Bruusgaard *et al.*, 2010) thus provides the cell with an additional biosynthetic capacity. Myonuclear accrual is also required for de novo hypertrophy (Egner *et al.*, 2016, 2017; Goh and Millay, 2017) in order to preserve muscle function (Goh *et al.*, 2019; Englund *et al.*, 2020b; Masschelein *et al.*, 2020). For example, a study by Goh *et al.* (2019) demonstrated that inhibition of myoblast fusogenicity caused exercise intolerance that abrogated hypertrophy, which has also been shown to disrupt transcriptional coordination within muscle fibers during exercise (Englund *et al.*, 2020a), pointing toward an obligatory requirement of nuclear donation via muscle stem cells for normal muscle growth.

Fusion and accretion of muscle stem cells also occur during developmental growth (White *et al.*, 2010; Yin *et al.*, 2013), and for the developing muscle fibers analyzed in Hansson *et al.* (2020a), maximal growth rates were proportional to DNA content but inversely proportional to the growing fiber volume, allowing fibers with more nuclei to grow faster than fibers with fewer nuclei. This even seems to be the case in animals that were genetically engineered to have fewer nuclei, although they did not reach the same absolute sizes (Cramer *et al.*, 2020; Hansson *et al.*, 2020a). Similar findings by Neurohr *et al.* (2019) demonstrate that maximal growth rates are related to ploidy levels in yeast strains (triploid > diploid > haploid). Because fibers at the very beginning of postnatal growth start with the same size (White *et al.*, 2010; Hansson *et al.*, 2020a), a fiber with a higher nuclear density can at least theoretically produce a system more concentrated in macromolecules due to the higher biosynthetic capacity. A system more concentrated in macromolecules may thus allow for faster assembly rates of intracellular structures (Goehring and Hyman, 2012). However, as each fiber grows, the pool of macromolecules is diminished in proportion to the growth rate and the increased cell volume adds to the effect of cytoplasmic dilution that may cause fibers to display growth rates that are inversely proportional to cytoplasmic volumes (Figure 4).

At the same time, this causes larger fibers to have, relative to their volume, fewer nuclei than smaller fibers and consequently must nurture a larger proportion of the cytoplasm.

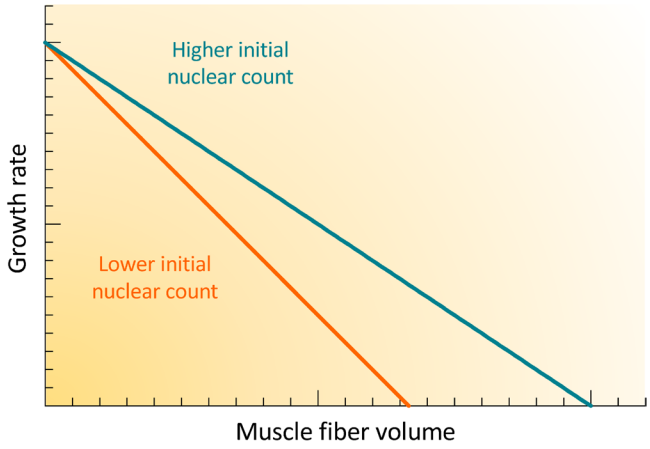

FIGURE 4: Growth rates in muscle fibers are inversely proportional to the cytoplasmic volume. The growth rates within muscle fibers during development or overload-induced hypertrophy are proportional to the nuclear number, causing the fiber with greater DNA content (green) to reach larger sizes compared with the fiber with lesser DNA content (orange). Theoretically, fibers stop growing when certain growth factors become too diluted.

Interestingly, the same growth pattern was also observed for muscle fibers that have excessively large myonuclear domain volumes after ablating myonuclear accretion (Cramer *et al.*, 2020), although the mice harboring these muscles underperformed physiologically. Why muscle fibers display this type of nonlinear growth is hitherto unknown, although as their size increases it is mechanistically paralleled by a decline in the abundance of the nucleolar transcription factor UBF and the concomitant decrease in RNA concentration during muscle maturation (Fiorotto *et al.*, 2014), both of which are imperative for regulating rRNA synthesis, protein content, and cell size (Hannan *et al.*, 2003; von Walden *et al.*, 2012). Thus, having large fiber domain volumes may result in a disproportionate cytoplasmic dilution that in proliferative cells has been associated with impaired cell function (Miettinen and Bjorklund, 2016; Miettinen *et al.*, 2017; Neurohr *et al.*, 2019). Below, we therefore elaborate on the physical constraints for which biological scaling is feasible during more detrimental conditions.

SCALING OF MUSCLE FIBERS DURING DISEASE AND AGING

Disturbance of myonuclear placement impairs muscle function, for instance, after mutations in the *Drosophila* larvae (Metzger *et al.*, 2012; Folker and Baylies, 2013) as well as during aging in mice (Bruusgaard *et al.*, 2006) and humans (Brack *et al.*, 2005; Cristea *et al.*, 2010). The study of myonuclear organization within muscle fibers of old mice (23 mo) by Bruusgaard *et al.* (2006) found that the myonuclear shape changed with age, from a more circular to more elongated shape, and that the myonuclei were distributed less regularly along the fiber. Age-related differences in the shape of human myonuclei have also been reported, as the nuclear envelope is typically more elongated with increased indentations at advanced age (Cristea *et al.*, 2010). Similarly, myonuclear distribution is disturbed in several myopathies, which leads to grave atrophy that is accompanied by myonuclear clustering. This might play a causative role in impairing function (Romero, 2010), as it may cause lacunas, regions within the muscle fiber having long transport distances (Hansson *et al.*, 2020b). Hence, the aggregation of myonuclei increases the severity of issues related to the transportation and distribution of macromolecules within the muscle fibers, which are exacerbated in large muscle fibers due to their larger myonuclear domain volumes (Omairi *et al.*, 2016). For example, regional differences in myonuclear domain sizes along the length of the fiber may be linked to irregular mitochondrial dysfunction and oxidative stress that occurs locally within muscle fibers (Wanagat *et al.*, 2001; Oldfors *et al.*, 2006), ultimately affecting the ability of muscles to generate force (D'Antona *et al.*, 2003).

As was pointed out previously, the total fiber surface area may constrain myonuclear productivity, as nutrients, oxygen, and growth factors all rely on the interaction with the fiber membrane to supply the cell with essential resources and activate cellular pathways. In terms of the supply, a fiber's capillary network plays a crucial role. A metric to determine the capillary supply area is to delineate a capillary domain area by portioning an area based on the equidistant boundaries between neighboring capillaries. Using capillary domains, as well as other methods as a proxy for a supply area (Kano *et al.*, 2002; Janacek *et al.*, 2009), it has been shown that the supply depends more heavily on the fiber size than on fiber type and oxidative capacity (Ahmed *et al.*, 1997; Wust *et al.*, 2009a,b; Bosutti *et al.*, 2015). Indeed, fiber growth and capillary supply are closely linked, because angiogenesis occurs simultaneously with overload-induced hypertrophy (Egginton *et al.*, 2011), while during age-related fiber atrophy of the human v. lateralis muscle, the number of capillaries per muscle fiber decreases (Frontera *et al.*, 2000; Croley *et al.*, 2005; Ryan *et al.*, 2006). This type of capillary rarefaction also occurs during disuse atrophy of the muscle fibers (Tyml and Mathieu-Costello, 2001).

The mitogenic vascular endothelial growth factor (VEGF) seems to bridge the communication between endothelial cells and satellite cells, as neutralizing VEGF with antibodies causes the proliferation of satellite cells to be reduced by at least 40% and up to 90% in some cases (Christov *et al.*, 2007; Abou-Khalil *et al.*, 2010). The study by Christov *et al.* (2007) also revealed that activated satellite cells could orstimulate endothelial cells to induce angiogenesis, while endothelial cells in return could stimulate myogenesis. Not only are satellite cells found in close vicinity of the capillaries (Christov *et al.*, 2007; Nederveen *et al.*, 2016) but the distance between the two cell types also increases in the old muscle (Nederveen *et al.*, 2016). Therefore, disorganization of myonuclei within fibers together with large cytoplasmic volumes per nucleus can influence transcriptional activity and protein synthesis, causing muscle fibers to deteriorate physiologically, while the natural decrease in satellite cell number during aging can hinder myonuclear replacement and support of the muscle fibers (Brack and Munoz-Canoves, 2016).

CONCLUDING REMARKS

Muscle biologists have long sought to understand size regulation in the highly malleable multinucleated skeletal muscle fiber. The more common reductionistic approach is without a doubt warranted to understand the molecular behavior of these cells, yet a more generalized approach can be important to obtain insights into details that eventually become too complex without a theorized holistic explanation. Herein we have combined current knowledge about myonuclear domains and muscle fiber size regulation with universal scaling laws originating from mononucleated cells and put it in a theorized framework as an approach to understand more about cell size regulation in multinucleated skeletal muscle fibers. We show with this framework that multinucleated muscle fibers adhere to the same general rules for size constraints as mononucleated cells. We propose that such a framework should be considered when investigating fiber size regulation under different circumstances such as during exercise, inactivity, disease, and age-related muscle loss, as this might aid the search for remedies against circumstances negatively

impacting muscle size and function. Importantly, the word "scaling" has been used to describe a size-related relationship more superficially in muscle biology, and by overlooking the scaling exponent, studies often fail to address whether the scaling behavior is linear, sublinear, or superlinear. Naively assuming the scaling of DNA content to fiber size to be linear may have profound effects on the interpretation of the data and its biological relevance to "size," which may further impact the design of therapeutic strategies to preserve muscle mass and function.

ACKNOWLEDGMENTS

Figures 1–3 were created with BioRender.com.

REFERENCES

Abou-Khalil R, Mounier R, Chazaud B (2010). Regulation of myogenic stem cell behavior by vessel cells: the "menage a trois" of satellite cells, periendothelial cells and endothelial cells. Cell Cycle 9, 892–896.

Ahmed SK, Egginton S, Jakeman PM, Mannion AF, Ross HF (1997). Is human skeletal muscle capillary supply modelled according to fibre size or fibre type? Exp Physiol 82, 231–234.

Albert R (2005). Scale-free networks in cell biology. J Cell Sci 118, 4947–4957.

Allen DL, Roy RR, Edgerton VR (1999). Myonuclear domains in muscle adaptation and disease. Muscle Nerve 22, 1350–1360.

Amodeo AA, Skotheim JM (2016). Cell-size control. Cold Spring Harb Perspect Biol 8, a019083.

Andersen JL, Gruschy-Knudsen T, Sandri C, Larsson L, Schiaffino S (1999). Bed rest increases the amount of mismatched fibers in human skeletal muscle. J Appl Physiol (1985) 86, 455–460.

Andersen JL, Schiaffino S (1997). Mismatch between myosin heavy chain mRNA and protein distribution in human skeletal muscle fibers. Am J Physiol 272, C1881–C1889.

Beardslee MA, Laing JG, Beyer EC, Saffitz JE (1998). Rapid turnover of connexin43 in the adult rat heart. Circ Res 83, 629–635.

Bertaux F, von Kugelgen J, Marguerat S, Shahrezaei V (2020). A bacterial size law revealed by a coarse-grained model of cell physiology. PLoS Comput Biol 16, e1008245.

Bosutti A, Egginton S, Barnouin Y, Ganse B, Rittweger J, Degens H (2015). Local capillary supply in muscle is not determined by local oxidative capacity. J Exp Biol 218, 3377–3380.

Brack AS, Bildsoe H, Hughes SM (2005). Evidence that satellite cell decrement contributes to preferential decline in nuclear number from large fibres during murine age-related muscle atrophy. J Cell Sci 118, 4813–4821.

Brack AS, Munoz-Canoves P (2016). The ins and outs of muscle stem cell aging. Skelet Muscle 6, 1.

Bruusgaard JC, Johansen IB, Egner IM, Rana ZA, Gundersen K (2010). Myonuclei acquired by overload exercise precede hypertrophy and are not lost on detraining. Proc Natl Acad Sci USA 107, 15111–15116.

Bruusgaard JC, Liestol K, Ekmark M, Kollstad K, Gundersen K (2003). Number and spatial distribution of nuclei in the muscle fibres of normal mice studied in vivo. J Physiol 551, 467–478.

Bruusgaard JC, Liestol K, Gundersen K (2006). Distribution of myonuclei and microtubules in live muscle fibers of young, middle-aged, and old mice. J Appl Physiol (1985) 100, 2024–2030.

Cadart C, Monnier S, Grilli J, Saez PJ, Srivastava N, Attia R, Terriac E, Baum B, Cosentino-Lagomarsino M, Piel M (2018). Size control in mammalian cells involves modulation of both growth rate and cell cycle duration. Nat Commun 9, 3275.

Cadart C, Venkova L, Recho P, Lagomarsino MC, Piel M (2019). The physics of cell-size regulation across timescales. Nat Phys 15, 993–1004.

Cantwell H, Nurse P (2019). Unravelling nuclear size control. Curr Genet 65, 1281–1285.

Chan YH, Marshall WF (2010). Scaling properties of cell and organelle size. Organogenesis 6, 88–96.

Cheek DB (1985). The control of cell mass and replication. The DNA unit—a personal 20-year study. Early Hum Dev 12, 211–239.

Cheek DB, Holt AB, Hill DE, Talbert JL (1971). Skeletal muscle cell mass and growth: the concept of the deoxiribonucleic acid unit. Pediatr Res 5, 312–328.

Christov C, Chretien F, Abou-Khalil R, Bassez G, Vallet G, Authier FJ, Bassaglia Y, Shinin V, Tajbakhsh S, Chazaud B, Gherardi RK (2007). Muscle satellite cells and endothelial cells: close neighbors and privileged partners. Mol Biol Cell 18, 1397–1409.

Clark PJ, Evans FC (1954). Distance to nearest neighbor as a measure of spatial relationships in populations. Ecology 35, 445–453.

Cramer AAW, Prasad V, Eftestol E, Song T, Hansson KA, Dugdale HF, Sadayappan S, Ochala J, Gundersen K, Millay DP (2020). Nuclear numbers in syncytial muscle fibers promote size but limit the development of larger myonuclear domains. Nat Commun 11, 6287.

Cristea A, Qaisar R, Edlund PK, Lindblad J, Bengtsson E, Larsson L (2010). Effects of aging and gender on the spatial organization of nuclei in single human skeletal muscle cells. Aging Cell 9, 685–697.

Croley AN, Zwetsloot KA, Westerkamp LM, Ryan NA, Pendergast AM, Hickner RC, Pofahl WE, Gavin TP (2005). Lower capillarization, VEGF protein, and VEGF mRNA response to acute exercise in the vastus lateralis muscle of aged vs. young women. J Appl Physiol (1985) 99, 1872–1879.

D'Antona G, Pellegrino MA, Adami R, Rossi R, Carlizzi CN, Canepari M, Saltin B, Bottinelli R (2003). The effect of ageing and immobilization on structure and function of human skeletal muscle fibres. J Physiol 552, 499–511.

da Silva Lopes K, Pietas A, Radke MH, Gotthardt M (2011). Titin visualization in real time reveals an unexpected level of mobility within and between sarcomeres. J Cell Biol 193, 785–798.

Demidenko ZN, Blagosklonny MV (2008). Growth stimulation leads to cellular senescence when the cell cycle is blocked. Cell Cycle 7, 3355–3361.

Denes LT, Kelley CP, Wang ET (2021). Microtubule-based transport is essential to distribute RNA and nascent protein in skeletal muscle. Nat Commun 12, 6079.

Di Biase V, Tuluc P, Campiglio M, Obermair GJ, Heine M, Flucher BE (2011). Surface traffic of dendritic CaV1.2 calcium channels in hippocampal neurons. J Neurosci 31, 13682–13694.

Dolezel J, Bartos J, Voglmayr H, Greilhuber J (2003). Nuclear DNA content and genome size of trout and human. Cytometry A 51, 127–128 [author reply, 129].

Egger M, Porzig H, Niggli E, Schwaller B (2005). Rapid turnover of the "functional" Na(+)-Ca2+ exchanger in cardiac myocytes revealed by an antisense oligodeoxynucleotide approach. Cell Calcium 37, 233–243.

Egginton S, Badr I, Williams J, Hauton D, Baan GC, Jaspers RT (2011). Physiological angiogenesis is a graded, not threshold, response. J Physiol 589, 195–206.

Egner IM, Bruusgaard JC, Gundersen K (2016). Satellite cell depletion prevents fiber hypertrophy in skeletal muscle. Development 143, 2898–2906.

Egner IM, Bruusgaard JC, Gundersen K (2017). An apparent lack of effect of satellite cell depletion on hypertrophy could be due to methodological limitations. Response to "Methodological issues limit interpretation of negative effects of satellite cell depletion on adult muscle hypertrophy." Development 144, 1365–1367.

Englund DA, Figueiredo VC, Dungan CM, Murach KA, Peck BD, Petrosino JM, Brightwell CR, Dupont AM, Neal AC, Fry CS, *et al*. (2020a). Satellite cell depletion disrupts transcriptional coordination and muscle adaptation to exercise. Function 2. zqaa033.

Englund DA, Murach KA, Dungan CM, Figueiredo VC, Vechetti IJ Jr, Dupont-Versteegden EE, McCarthy JJ, Peterson CA (2020b). Depletion of resident muscle stem cells negatively impacts running volume, physical function, and muscle fiber hypertrophy in response to lifelong physical activity. Am J Physiol Cell Physiol 318, C1178–C1188.

Figueiredo VC, McCarthy JJ (2019). Regulation of ribosome biogenesis in skeletal muscle hypertrophy. Physiology (Bethesda) 34, 30–42.

Fiorotto ML, Davis TA, Reeds PJ (2000). Regulation of myofibrillar protein turnover during maturation in normal and undernourished rat pups. Am J Physiol Regul Integr Comp Physiol 278, R845–R854.

Fiorotto ML, Davis TA, Sosa HA, Villegas-Montoya C, Estrada I, Fleischmann R (2014). Ribosome abundance regulates the recovery of skeletal muscle protein mass upon recuperation from postnatal undernutrition in mice. J Physiol 592, 5269–5286.

Folker ES, Baylies MK (2013). Nuclear positioning in muscle development and disease. Front Physiol 4, 363.

Frontera WR, Hughes VA, Fielding RA, Fiatarone MA, Evans WJ, Roubenoff R (2000). Aging of skeletal muscle: a 12-yr longitudinal study. J Appl Physiol (1985) 88, 1321–1326.

Gastner MT, Newman ME (2006). Optimal design of spatial distribution networks. Phys Rev E 74, 016117.

Gilarranz LJ (2020). Generic emergence of modularity in spatial networks. Sci Rep 10, 8708.

Gillooly JF, Hein A, Damiani R (2015). Nuclear DNA content varies with cell size across human cell types. Cold Spring Harb Perspect Biol 7, a019091.
Goehring NW, Hyman AA (2012). Organelle growth control through limiting pools of cytoplasmic components. Curr Biol 22, R330–R339.
Goh Q, Millay DP (2017). Requirement of myomaker-mediated stem cell fusion for skeletal muscle hypertrophy. eLife 6, e20007.
Goh Q, Song T, Petrany MJ, Cramer AA, Sun C, Sadayappan S, Lee SJ, Millay DP (2019). Myonuclear accretion is a determinant of exercise-induced remodeling in skeletal muscle. eLife 8, e44876.
Goldspink DF (1977). The influence of activity on muscle size and protein turnover. J Physiol 264, 283–296.
Gundersen K (2011). Excitation-transcription coupling in skeletal muscle: the molecular pathways of exercise. Biol Rev Camb Philos Soc 86, 564–600.
Hall ZW, Ralston E (1989). Nuclear domains in muscle cells. Cell 59, 771–772.
Hannan KM, Brandenburger Y, Jenkins A, Sharkey K, Cavanaugh A, Rothblum L, Moss T, Poortinga G, McArthur GA, Pearson RB, Hannan RD (2003). mTOR-dependent regulation of ribosomal gene transcription requires S6K1 and is mediated by phosphorylation of the carboxy-terminal activation domain of the nucleolar transcription factor UBF. Mol Cell Biol 23, 8862–8877.
Hansson KA, Eftestol E, Bruusgaard JC, Juvkam I, Cramer AW, Malthe-Sorenssen A, Millay DP, Gundersen K (2020a). Myonuclear content regulates cell size with similar scaling properties in mice and humans. Nat Commun 11, 6288.
Hansson KA, Solbra AV, Gundersen K, Bruusgaard JC (2020b). Computational assessment of transport distances in living skeletal muscle fibers studied in situ. Biophys J 119, 2166–2178.
Hargrove JL, Schmidt FH (1989). The role of mRNA and protein stability in gene expression. FASEB J 3, 2360–2370.
Harris AJ, Duxson MJ, Butler JE, Hodges PW, Taylor JL, Gandevia SC (2005). Muscle fiber and motor unit behavior in the longest human skeletal muscle. J Neurosci 25, 8528–8533.
Ishibashi T, Ruggeri ZM, Harker LA, Burstein SA (1986). Separation of human megakaryocytes by state of differentiation on continuous gradients of Percoll: size and ploidy analysis of cells identified by monoclonal antibody to glycoprotein IIb/IIIa. Blood 67, 1286–1292.
Isaacs WB, Kim IS, Struve A, Fulton AB (1989). Biosynthesis of titin in cultured skeletal muscle cells. J Cell Biol 109, 2189–2195.
Janacek J, Cebasek V, Kubinova L, Ribaric S, Erzen I (2009). 3D visualization and measurement of capillaries supplying metabolically different fiber types in the rat extensor digitorum longus muscle during denervation and reinnervation. J Histochem Cytochem 57, 437–447.
Kafri M, Metzl-Raz E, Jona G, Barkai N (2016). The cost of protein production. Cell Rep 14, 22–31.
Kann F (1957). [Diameter and number of muscle fibers in various cross section levels of sartorius muscle in man.]. Acta Anat (Basel) 30, 351–357.
Kano Y, Shimegi S, Furukawa H, Matsudo H, Mizuta T (2002). Effects of aging on capillary number and luminal size in rat soleus and plantaris muscles. J Gerontol A Biol Sci Med Sci 57, B422–B427.
Katz ZB, English BP, Lionnet T, Yoon YJ, Monnier N, Ovryn B, Bathe M, Singer RH (2016). Mapping translation "hot-spots" in live cells by tracking single molecules of mRNA and ribosomes. eLife 5, e10415.
Kay J (1978). Intracellular protein degradation. Biochem Soc Trans 6, 789–797.
Kim MJ, O'Connor MB (2021). Drosophila Activin signaling promotes muscle growth through InR/TORC1-dependent and -independent processes. Development 148, dev190868.
Lanz MC, Zatulovskiy E, Swaffer MP, Zhang L, Ilerten I, Zhang S, You DS, Marinov G, McAlpine P, Elias JE, Skotheim JM (2022). Increasing cell size remodels the proteome and promotes senescence. Mol Cell 82, 3255–3269.e8.
Lee MV, Topper SE, Hubler SL, Hose J, Wenger CD, Coon JJ, Gasch AP (2011). A dynamic model of proteome changes reveals new roles for transcript alteration in yeast. Mol Syst Biol 7, 514.
Li GW, Burkhardt D, Gross C, Weissman JS (2014). Quantifying absolute protein synthesis rates reveals principles underlying allocation of cellular resources. Cell 157, 624–635.
Lin J, Amir A (2018). Homeostasis of protein and mRNA concentrations in growing cells. Nat Commun 9, 4496.
Liu Y, Beyer A, Aebersold R (2016). On the dependency of cellular protein levels on mRNA abundance. Cell 165, 535–550.
Luby-Phelps K (2013). The physical chemistry of cytoplasm and its influence on cell function: an update. Mol Biol Cell 24, 2593–2596.
Manhart A, Windner S, Baylies M, Mogilner A (2018). Mechanical positioning of multiple nuclei in muscle cells. PLoS Comput Biol 14, e1006208.
Marguerat S, Bahler J (2012). Coordinating genome expression with cell size. Trends Genet 28, 560–565.
Masschelein E, D'Hulst G, Zvick J, Hinte L, Soro-Arnaiz I, Gorski T, von Meyenn F, Bar-Nur O, De Bock K (2020). Exercise promotes satellite cell contribution to myofibers in a load-dependent manner. Skelet Muscle 10, 21.
McMahon TA, Bonner JT (1983). On Size and Life, New York: Scientific American Library, distributed by W.H. Freeman.
Merlie JP, Sanes JR (1985). Concentration of acetylcholine receptor mRNA in synaptic regions of adult muscle fibres. Nature 317, 66–68.
Metzger T, Gache V, Xu M, Cadot B, Folker ES, Richardson BE, Gomes ER, Baylies MK (2012). MAP and kinesin-dependent nuclear positioning is required for skeletal muscle function. Nature 484, 120–124.
Metzl-Raz E, Kafri M, Yaakov G, Barkai N (2020). Gene transcription as a limiting factor in protein production and cell growth. G3 (Bethesda) 10, 3229–3242.
Miettinen TP, Bjorklund M (2015). Mevalonate pathway regulates cell size homeostasis and proteostasis through autophagy. Cell Rep 13, 2610–2620.
Miettinen TP, Bjorklund M (2016). Cellular allometry of mitochondrial functionality establishes the optimal cell size. Dev Cell 39, 370–382.
Miettinen TP, Caldez MJ, Kaldis P, Bjorklund M (2017). Cell size control - a mechanism for maintaining fitness and function. Bioessays 39, doi: 10.1002/bies.201700058.
Mishra P, Varuzhanyan G, Pham AH, Chan DC (2015). Mitochondrial dynamics is a distinguishing feature of skeletal muscle fiber types and regulates organellar compartmentalization. Cell Metab 22, 1033–1044.
Mitchison JM (2003). Growth during the cell cycle. Int Rev Cytol 226, 165–258.
Morin A, Stantzou A, Petrova ON, Hildyard J, Tensorer T, Matouk M, Petkova MV, Richard I, Manoliu T, Goyenvalle A, *et al*. (2023). Dystrophin myonuclear domain restoration governs treatment efficacy in dystrophic muscle. Proc Natl Acad Sci USA 120, e2206324120.
Nederveen JP, Joanisse S, Snijders T, Ivankovic V, Baker SK, Phillips SM, Parise G (2016). Skeletal muscle satellite cells are located at a closer proximity to capillaries in healthy young compared with older men. J Cachexia Sarcopenia Muscle 7, 547–554.
Neurohr GE, Terry RL, Lengefeld J, Bonney M, Brittingham GP, Moretto F, Miettinen TP, Vaites LP, Soares LM, Paulo JA, *et al*. (2019). Excessive cell growth causes cytoplasm dilution and contributes to senescence. Cell 176, 1083–1097.e1018.
Nevalainen M, Kaakinen M, Metsikko K (2013). Distribution of mRNA transcripts and translation activity in skeletal myofibers. Cell Tissue Res 353, 539–548.
Niklas KJ (2015). A phyletic perspective on cell growth. Cold Spring Harb Perspect Biol 7, a019158.
Okie JG (2013). General models for the spectra of surface area scaling strategies of cells and organisms: fractality, geometric dissimilitude, and internalization. Am Nat 181, 421–439.
Oldfors A, Moslemi AR, Jonasson L, Ohlsson M, Kollberg G, Lindberg C (2006). Mitochondrial abnormalities in inclusion-body myositis. Neurology 66, S49–S55.
Omairi S, Matsakas A, Degens H, Kretz O, Hansson KA, Solbra AV, Bruusgaard JC, Joch B, Sartori R, Giallourou N, *et al*. (2016). Enhanced exercise and regenerative capacity in a mouse model that violates size constraints of oxidative muscle fibres. eLife 5, e16940.
Padovan-Merhar O, Nair GP, Biaesch AG, Mayer A, Scarfone S, Foley SW, Wu AR, Churchman LS, Singh A, Raj A (2015). Single mammalian cells compensate for differences in cellular volume and DNA copy number through independent global transcriptional mechanisms. Mol Cell 58, 339–352.
Papadopoulos S, Endeward V, Revesz-Walker B, Jurgens KD, Gros G (2001). Radial and longitudinal diffusion of myoglobin in single living heart and skeletal muscle cells. Proc Natl Acad Sci USA 98, 5904–5909.
Papadopoulos S, Jurgens KD, Gros G (2000). Protein diffusion in living skeletal muscle fibers: dependence on protein size, fiber type, and contraction. Biophys J 79, 2084–2094.
Pavlath GK, Rich K, Webster SG, Blau HM (1989). Localization of muscle gene products in nuclear domains. Nature 337, 570–573.
Pilling AD, Horiuchi D, Lively CM, Saxton WM (2006). Kinesin-1 and Dynein are the primary motors for fast transport of mitochondria in Drosophila motor axons. Mol Biol Cell 17, 2057–2068.
Pinheiro H, Pimentel MR, Sequeira C, Oliveira LM, Pezzarossa A, Roman W, Gomes ER (2021). mRNA distribution in skeletal muscle is associated with mRNA size. J Cell Sci 134, jcs256388.

Ralston E, Hall ZW (1992). Restricted distribution of mRNA produced from a single nucleus in hybrid myotubes. J Cell Biol 119, 1063–1068.
Rhind N (2021). Cell-size control. Curr Biol 31, R1414–R1420.
Roman W, Gomes ER (2018). Nuclear positioning in skeletal muscle. Semin Cell Dev Biol 82, 51–56.
Romero NB (2010). Centronuclear myopathies: a widening concept. Neuromuscul Disord 20, 223–228.
Ryan NA, Zwetsloot KA, Westerkamp LM, Hickner RC, Pofahl WE, Gavin TP (2006). Lower skeletal muscle capillarization and VEGF expression in aged vs. young men. J Appl Physiol (1985) 100, 178–185.
Sartori R, Milan G, Patron M, Mammucari C, Blaauw B, Abraham R, Sandri M (2009). Smad2 and 3 transcription factors control muscle mass in adulthood. Am J Physiol Cell Physiol 296, C1248–C1257.
Schiaffino S, Mammucari C (2011). Regulation of skeletal muscle growth by the IGF1-Akt/PKB pathway: insights from genetic models. Skelet Muscle 1, 4.
Schiaffino S, Reggiani C (2011). Fiber types in mammalian skeletal muscles. Physiol Rev 91, 1447–1531.
Schmidt-Nielsen K (1984). Scaling, Why Is Animal Size So Important?, Cambridge, UK: Cambridge University Press.
Schott DH, Collins RN, Bretscher A (2002). Secretory vesicle transport velocity in living cells depends on the myosin-V lever arm length. J Cell Biol 156, 35–39.
Schwanhausser B, Busse D, Li N, Dittmar G, Schuchhardt J, Wolf J, Chen W, Selbach M (2011). Global quantification of mammalian gene expression control. Nature 473, 337–342.
Soh S, Banaszak M, Kandere-Grzybowska K, Grzybowski BA (2013). Why cells are microscopic: a transport-time perspective. J Phys Chem Lett 4, 861–865.
Spahr PF (1962). Amino acid composition of ribosomes from Escherichia coli. J Mol Biol 4, 395–406.
Taylor-Weiner H, Grigsby CL, Ferreira DMS, Dias JM, Stevens MM, Ruas JL, Teixeira AI (2020). Modeling the transport of nuclear proteins along single skeletal muscle cells. Proc Natl Acad Sci USA 117, 2978–2986.
Tyml K, Mathieu-Costello O (2001). Structural and functional changes in the microvasculature of disused skeletal muscle. Front Biosci 6, D45–D52.
von Walden F (2019). Ribosome biogenesis in skeletal muscle: coordination of transcription and translation. J Appl Physiol (1985) 127, 591–598.
von Walden F, Casagrande V, Ostlund Farrants AK, Nader GA (2012). Mechanical loading induces the expression of a Pol I regulon at the onset of skeletal muscle hypertrophy. Am J Physiol Cell Physiol 302, C1523–C1530.
Wallace RA, Misulovin Z, Etkin LD (1981). Full-grown oocytes from Xenopus laevis resume growth when placed in culture. Proc Natl Acad Sci USA 78, 3078–3082.
Wanagat J, Cao Z, Pathare P, Aiken JM (2001). Mitochondrial DNA deletion mutations colocalize with segmental electron transport system abnormalities, muscle fiber atrophy, fiber splitting, and oxidative damage in sarcopenia. FASEB J 15, 322–332.
White RB, Bierinx AS, Gnocchi VF, Zammit PS (2010). Dynamics of muscle fibre growth during postnatal mouse development. BMC Dev Biol 10, 21.
Windner SE, Manhart A, Brown A, Mogilner A, Baylies MK (2019). Nuclear scaling is coordinated among individual nuclei in multinucleated muscle fibers. Dev Cell 49, 48–62.e43.
Wust RC, Gibbings SL, Degens H (2009a). Fiber capillary supply related to fiber size and oxidative capacity in human and rat skeletal muscle. Adv Exp Med Biol 645, 75–80.
Wust RC, Jaspers RT, van Heijst AF, Hopman MT, Hoofd LJ, van der Laarse WJ, Degens H (2009b). Region-specific adaptations in determinants of rat skeletal muscle oxygenation to chronic hypoxia. Am J Physiol Heart Circ Physiol 297, H364–H374.
Xiao S, Zhang J, Romero MM, Smith KN, Shea LD, Woodruff TK (2015). In vitro follicle growth supports human oocyte meiotic maturation. Sci Rep 5, 17323.
Yin H, Price F, Rudnicki MA (2013). Satellite cells and the muscle stem cell niche. Physiol Rev 93, 23–67.
Young RB, Schneible PA (1984). Myosin heavy chain concentration, synthesis rate and degradation rate in normal and dystrophic chicken muscle cells in culture. Eur J Cell Biol 34, 75–79.
Zak R, Martin AF, Prior G, Rabinowitz M (1977). Comparison of turnover of several myofibrillar proteins and critical evaluation of double isotope method. J Biol Chem 252, 3430–3435.
Zur H, Cohen-Kupiec R, Vinokour S, Tuller T (2020). Algorithms for ribosome traffic engineering and their potential in improving host cells' titer and growth rate. Sci Rep 10, 21202.